

## COMPUTATIONAL SIMULATION OF INDOORS TEMPERATURE FIELD: COMPARATIVE STUDY BETWEEN THE APLICATION OF SHORT AND LONG WIND-CATCH

Patricia R C Drach

Federal University of the Rio de Janeiro – Post-graduate Program in Urbanism of the  
School of Architecture and Urbanism - PROURB/FAU/UFRJ, Rio de Janeiro, Brazil

### ABSTRACT

Aiming to study the temperature field changes, the House VI project was checked. This house is located in Vila37, Rio de Janeiro, Brazil, a dead-end small street with only one inlet/outlet. In the houses of Vila37, the indoor ventilation is restricted to the facade windows. Giving the impossibility of introducing cross-ventilation in a traditional way, a short wind-catch was previously added with positive results; therefore, simulations with long wind-catch are being carried out. The analysis started by solving the air-circulation problem by using a finite element method and after, with the wind fields added, the heat transfer problem was analysed. The results obtained were evaluated and compared with the previous ones.

### INTRODUCTION

This study focuses on a specific town, the city of Rio de Janeiro. This city is located in a region of tropical climate, therefore hot. Between the years of 1872 and 1890, the urban population in Rio de Janeiro city almost doubled, reaching an increase of approximately 90% in only 18 years. A great migration of the rural population - mainly of former-slaves - had turned the city into an enormous informal job market and the main economical and financial centre of the country, in spite of the downtowns possession of typical characteristics of a colony (r, von der Weid, 2004).

The enormous growth in population impelled the expansion towards suburban areas and it provoked an increase in the demand for houses. Great part of the labouring population either lived in “vilas” (a dead-end small street with only one inlet/outlet) built by the company in which they worked or at improvised slums. Despite the fact that most “vilas” suffered alterations, mainly enlargements because the residences were usually very small, some of them still survive.

Vila 37 was built in the year of 1890 and is located in the neighbourhood of Catete, in Rio de Janeiro city, which has its history intimately linked to the cities very history (p.r.c. Drach, 2007). Figure 1 shows the photo of the entire original project and Figures 2(a) and 2(b) present the plants of the house pattern and of the location of the group of houses where it is possible to observe how the houses were very small

and that there was no space around them. They had originally just one room, one corridor, one bedroom and kitchen (Figure 2(a)). In agreement with old residents, the bathroom was located in the internal small street of the “vila” and it was collective in use and as a place for clothes washing. These documents were obtained in 2006 through the General Archive of Rio de Janeiro City – AGCRJ.

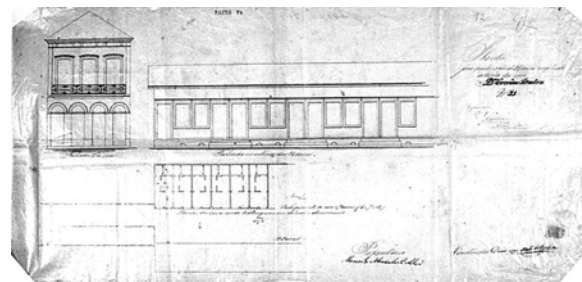


*Figure 1 Photo of the original document (1890) obtained from General Archive of Rio de Janeiro City – AGCRJ.*

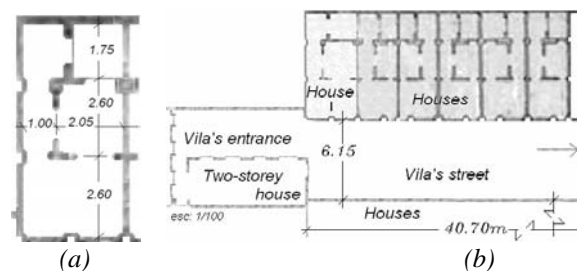


*Figure 2 Original details (1890): house pattern plan (a) and house group location (b).*

Through the years, many buildings of these areas of the city were demolished giving place to new and taller buildings. Later on, the embankment of Flamengo Beach was made meaning that these houses found themselves more distant from the sea.

As the houses were indeed very small, their inhabitants were left with no other option than to enlarge their homes vertically and now, some of the houses already have four floors. Nowadays these houses and the internal small street have been suffering a decrease of air circulation and the residents suffer from thermal discomfort mainly in the hottest hours of the day.

Aiming to analyze the changes that took place in the ventilation of these confined spaces, the project of House VI was checked. In this house with three-floors the ventilation is restricted to the windows in the facade. The plans of the three-floors can be observed in Figure 3, and the sections and the facade in Figure 4. These sketches are reproductions of the originals from August 2000 and are filed at the Secretaria Municipal de Urbanismo (Urbanization District Secretariat - Division of Property and Constructions Bureau) of Rio de Janeiro City.

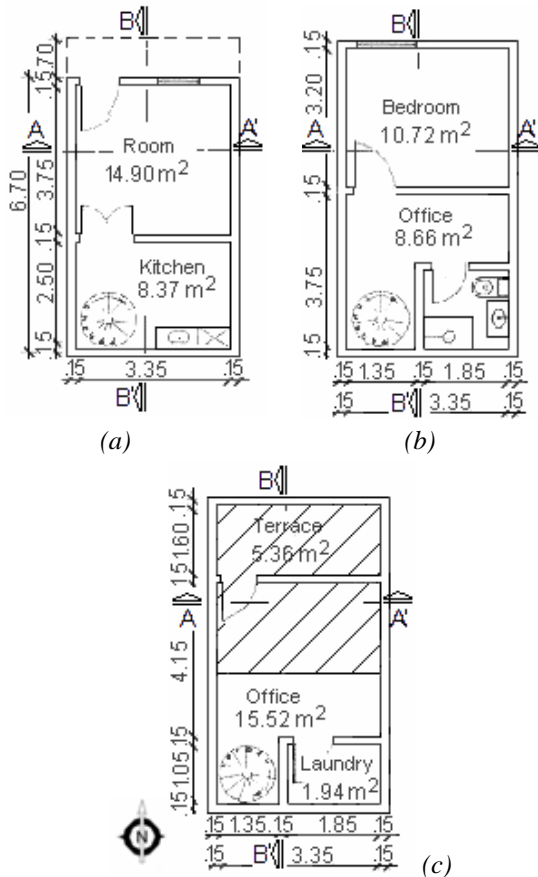


Figure 3 Plans of the three floors; first-floor (a), second-floor (b) and third-floor (c).

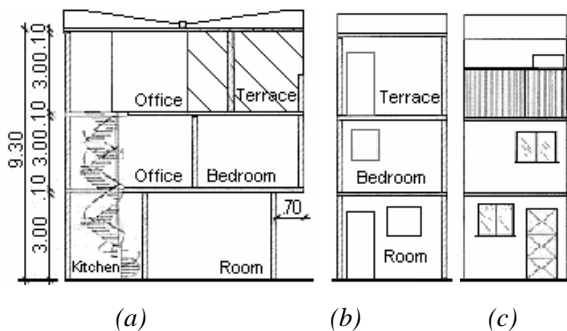


Figure 4 Sections and facade; section AA (a), section BB (b) and facade (c).

In this house, it is difficult to think about introduction of cross-ventilation in a traditional way. So we need to concentrate our focus on conscious and unusual

ways to introduce cross-ventilation into the design. Seeking to improve the thermal sensation especially on the third floor in a previous study (p.r.c. Drach and j. Karam F., 2008) the application of a short wind-catch that has openings only on this floor was tested. The results obtained made possible the observation the introduction of the wind-catch, therefore the insertion of cross ventilation brought about won in quality for the indoor space and they were encouraging and brought vitality to test the introduction of a long wind-catch that crosses the entire construction and has openings on all of the floors. In Figure 5 it is possible to see the original project (a) and the changes proposed (b and c) with the introduction of wind-catchers, drawn in red. The wind-catchers are facing the main wind and they are able to catch the air at a higher level, where it is cooler, faster and cleaner. The introduction of cross-ventilation allows not only indoor air circulation but also the ventilation towards the vila central street and in the opposite direction. The wind-catch can also help air and temperature exchanges, acting as an escape tower that exhausts the indoor heated air.

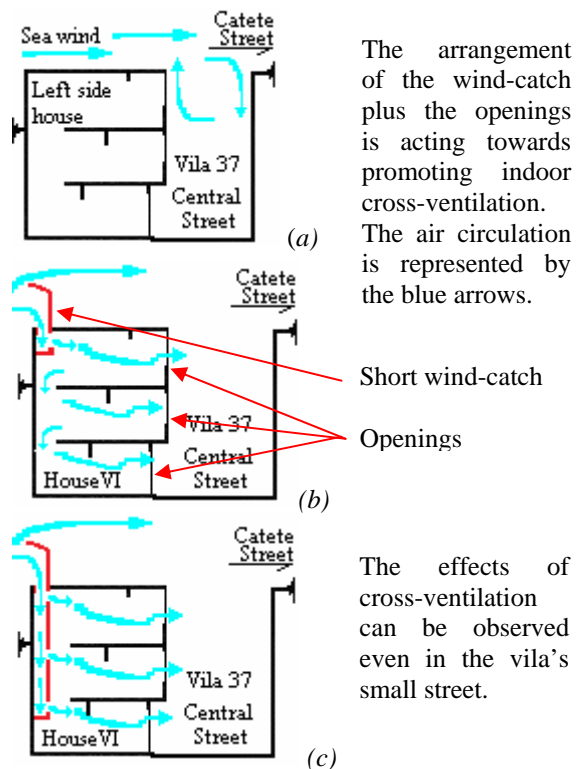


Figure 5 The original project (a) and the changes proposed (b and c) with the introduction of wind catchers.

Besides scarce ventilation, this pavement receives solar radiation directly. The interference of incident solar radiation on the flat roof was also considered, taking into account its respective materials. The thermal changes between outdoor and indoor environments include a solar gain factor related to

three specific hours; 7 a.m., 12 a.m., 4 p.m. and also includes no gain factor in one of the cases: at night. Computational simulations were carried out for this new case.

The meshes generated for the computational simulation comprise areas bigger than the ones on the plans, by doing this we can impose boundary conditions on the border of the meshes and leave the velocities and temperatures unknown at the entrances of the plans. So the velocities and temperatures could be determined by the solution of air circulation and thermal problems. The analysis starts by solving the air circulation problem to determine the wind fields, using a mixed stabilized finite element method - Petrov-Galerkin type - applied to the full Navier-Stokes equations written in velocity and pressure variables (l.p. Franca and s.l. Frey, 1992). Then, with these wind fields, using a stabilized finite element method - Streamline Up-Wind Petrov-Galerkin (SUPG) (a. Brooks and t.j.r. Hughes, 1982), the heat transfer problem, taking into account the heat conduction and convection, was solved and analyzed. The results obtained with the new scenario (with long wind-catch) are compared with the ones of the previous study (without and with short wind-catch). These computational results suggest that the use of a wind-catch associated with an appropriate arrangement of openings deserves more attention and research because they show an improvement in air circulation and an ability to promote cooling.

## MATHEMATICAL FORMULATION

The problem of air circulation and heat transfer can be modelled through mass, momentum and energy conservation equations. Assuming incompressibility, the mathematical formulation for the general problem can be written as: Find  $\mathbf{u}$ ,  $p$  and  $\theta$  satisfying the following system,

$$\operatorname{div}(\mathbf{u})=0, \text{ in } \Omega \times [0, T], \quad (1)$$

$$\rho \frac{\partial \mathbf{u}}{\partial t} + \rho(\nabla \mathbf{u})\mathbf{u} - 2\mu \operatorname{div} \varepsilon(\mathbf{u}) + \nabla p + \rho \mathbf{g} \beta(\theta - \theta_\infty) = 0, \text{ in } \Omega \times [0, T], \quad (2)$$

$$\rho c_p \frac{\partial \theta}{\partial t} + \rho c_p \mathbf{u}(\nabla \theta) - k \operatorname{div} \nabla \theta = 0, \text{ in } \Omega \times [0, T], \quad (3)$$

$$\begin{aligned} \nabla \mathbf{u} \bar{\mathbf{n}} &= 0 \text{ in } \Gamma_v \times [0, T], \mathbf{u}(\mathbf{x}, t) = \bar{\mathbf{u}}(\mathbf{x}, t) \text{ in } \Gamma_u \times [0, T], \mathbf{u}(\mathbf{x}, 0) = \mathbf{u}_0 \text{ in } \Omega \times [0, T], \\ k \nabla \theta \bar{\mathbf{n}} &= 0 \text{ in } \Gamma_a \times [0, T], \theta(\mathbf{x}, t) = \bar{\theta} \text{ in } \Gamma_c \times [0, T] \text{ and } \theta(\mathbf{x}, 0) = \theta_0(\mathbf{x}) \text{ in } \Omega \end{aligned}$$

where:

$\mathbf{u} = \mathbf{u}(\mathbf{x}, t)$  is the velocity vector,  $p = p(\mathbf{x}, t)$  is the pressure,  $\theta = \theta(\mathbf{x}, t)$  is the temperature,  $\mu$  is the viscosity,  $\rho$  is the density,  $k$  is the thermal conductivity,  $\theta_\infty$  is the reference temperature,  $\bar{\mathbf{n}}$  is the normal vector,  $c_p$  is the specific heat,  $\beta$  is the coefficient of thermal expansion,  $\mathbf{g}$  is the gravity vector,  $\varepsilon(\mathbf{u}) = \frac{1}{2}(\nabla \mathbf{u} + \nabla \mathbf{u}^T)$ ,  $\Omega$  is the bounded domain

with boundary  $\Gamma = \Gamma_u \cup \Gamma_v = \Gamma_c \cup \Gamma_d$  with  $\Gamma_u \cap \Gamma_v = \Gamma_c \cap \Gamma_d = \emptyset$  and the time  $t \in [0, T]$ .

The term  $\rho \mathbf{g} \beta(\theta - \theta_\infty)$  allows the coupling of the air circulation and the heat transfer problems.

## METHODS

For the air circulation problem the numerical solutions are here obtained by a stabilized mixed finite element method. This method allows us to deal with the difficulties that come from the first equation system, Equations (1) and (2): the difficulty in constructing approximation spaces for problems with internal constraint; non-linearities of the convective type and numerical instabilities when advection effects are dominant. Here, a Petrov-Galerkin type method (l.p. Franca and s.l. Frey, 1992) was implemented and applied to analyze indoor air circulation cases, ensuring stability for dominant advection and for the internal constraint. In the case of a heat transfer problem a stabilized finite element method was implemented - Streamline Up-wind Petrov-Galerkin (SUPG) (a. Brooks and t.j.r. Hughes, 1982).

Being  $L^2$  and  $H^1$  the usual Hilbert spaces and  $R_l^h$  the Lagrange polynomial space of the degree  $l$  and class  $C^0$ . Then, defining the following approximation spaces;

$$V_h = \{ \mathbf{u}_h \in (H_0^1(\Omega) \cap R_l^h(\Omega))^2, \mathbf{u}_h(\mathbf{x}, t) = \bar{\mathbf{u}}_h(\mathbf{x}, t) \text{ in } \Gamma_u \} \subset (H^1(\Omega))^2,$$

$$V_h^0 = \{ \mathbf{v}_h \in (H_0^1(\Omega) \cap R_l^h(\Omega))^2, \mathbf{v}_h(\mathbf{x}, t) = 0 \text{ in } \Gamma_u \} \subset (H^1(\Omega))^2,$$

$$P^h = \{ p_h \in (L^2(\Omega) \cap R_l^h(\Omega)); \int_\Omega p_h \bar{\alpha} \Omega = 0 \} \subset (L^2(\Omega)),$$

$$S^h = \{ \theta_h | \theta_h(\mathbf{x}, t) \in (H^1(\Omega) \cap R_l^h(\Omega)), \theta_h(\mathbf{x}, t) = \bar{\theta}_h(\mathbf{x}, t) \text{ in } \Gamma_c \} \subset (H^1(\Omega)),$$

$$S_h^0 = \{ s_h | s_h(\mathbf{x}, t) \in (H^1(\Omega) \cap R_l^h(\Omega)), s_h(\mathbf{x}, t) = 0 \text{ in } \Gamma_c \} \subset (H^1(\Omega)).$$

with the usual norm,

$$\|\mathbf{u}\|_1^2 = \|\mathbf{u}\|_0^2 + \|\nabla \mathbf{u}\|_0^2 \text{ of } H^1 \text{ and } \|p\| = \|p\|_0 \text{ of } L^2.$$

The wind field can be determined by solving the following formulation:

Find  $\{\mathbf{u}^h, p^h\} \in V^h \times P^h$  satisfying the following system

$$B(\mathbf{u}_h, p_h; \mathbf{v}_h, q_h) = 0, \forall (\mathbf{v}_h, q_h) \in V_h^0 \times P_h, \text{ where:}$$

$$B(\mathbf{u}_h, p_h; \mathbf{v}_h, q_h) = \left( \frac{\partial \mathbf{u}_h}{\partial t}, \mathbf{v}_h \right) + \left( (\nabla \mathbf{u}_h) \mathbf{a}_h, \mathbf{v}_h \right) + 2\nu \left( \varepsilon(\mathbf{u}_h), \varepsilon(\mathbf{v}_h) \right) +$$

$$\left( q_h, \operatorname{div}(\mathbf{u}_h) \right) - \left( p_h, \operatorname{div}(\mathbf{v}_h) \right) + \left( \operatorname{div}(\mathbf{u}_h), \delta_2 \operatorname{div}(\mathbf{v}_h) \right) +$$

$$\delta_1 \sum_{e=1}^{Nel} \left( \frac{\partial \mathbf{u}_h}{\partial t} + (\nabla \mathbf{u}_h) \mathbf{a}_h - 2\nu \operatorname{div} \varepsilon(\mathbf{u}_h) + \nabla p_h - \mathbf{g} \beta(\theta - \theta_\infty), \right.$$

$$\left. \left( (\nabla \mathbf{v}_h) \mathbf{a}_h - 2\nu \operatorname{div} \varepsilon(\mathbf{v}_h) + \nabla q_h \right) \right)_h + \gamma(P_h, q_h),$$

$$\forall \mathbf{v}_h \in V_h^0 \text{ e } q_h \in P_h.$$

with  $\gamma \ll 1$  and  $\delta_1$  and  $\delta_2$  stabilized parameters suggested by Franca and Frey (l.p. Franca and s.l. Frey, 1992)

And find  $\theta(\mathbf{x},t)$  satisfying the following system:

$$\left(\frac{\partial \theta_h}{\partial t}, s_h\right) + (k \nabla \theta_h, \nabla s_h) + (\mathbf{u} \cdot \nabla \theta_h, s_h) + \sum_{e=1}^{N_e} \left( \tau, \left( \left( \frac{\partial \theta_h}{\partial t} \right) - k \Delta \theta_h + \mathbf{u} \cdot \nabla \theta_h \right) \right)_h = 0, \forall s_h \in S_h^0$$

With  $\tau = \tilde{k} \mathbf{u} \cdot \nabla s_h$ , the SUPG stabilized parameters suggested by Brooks and Hughes (a. Brooks and t.j.r. Hughes, 1982). The time discretization has been done by backward Euler finite differences.

## SIMULATIONS

Meshes were generated with linear triangular elements and their collective dimensions comprise areas bigger than the ones in the plans as in Figure 6(a). This was in order to impose the boundary conditions on their borders and to leave unknown the velocities and the temperatures at the entrances, so, those variables can be determined by the solution of the problem. The mesh detail of the other two scenarios can be observed in Figures 6(b) and 6(c).

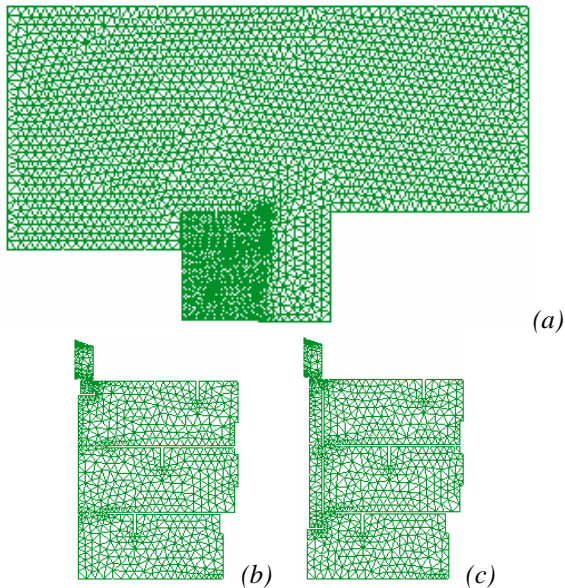


Figure 6 Original project whole mesh (a) and mesh details: short (b) and long wind-catch (c).

To test the situation even with low winds the boundary conditions adopted for outdoor wind were 1 m/s. The outdoor temperature of 31°C was selected, that corresponds approximately to the one of the February average, which is amongst the highest temperatures observed in Rio de Janeiro city. This value was selected from data at the Instituto Nacional de Meteorologia – INMET (Meteorology National Institute). For the indoor temperature, 33°C was taken as a basis. The sketch in Figure 7 shows the

boundary and initial conditions adopted. The arrow on the top of the figures indicates outdoor wind direction and intensity. The initial temperatures are indicated inside the squares.

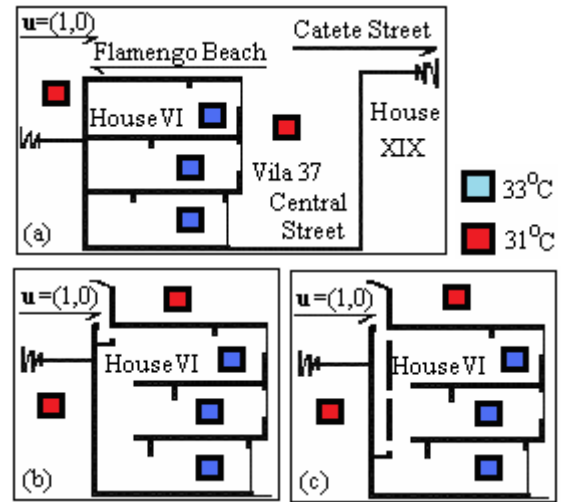


Figure 7 Boundary and initial conditions adopted for the original project (a), the scenario with short wind-catch and the new scenario (c).

To take into account the interference of the incident solar radiation and of the roof material on indoor temperatures, a temperature value was prescribed in the covering flagstone outline that was defined based on the studies of Frota and Shiffer (a.b. Frota and s.r. Shiffer, 1988). The calculation of the thermal flux intensity was made by the equation:

$$q = K \left( t_e + \frac{\alpha I_g}{h_e} - t_i \right),$$

where  $K$  is the global coefficient of thermal transmission,  $t_e$  is the outdoor temperature,  $t_i$  is the indoor temperature,  $\alpha$  is the solar absorption coefficient of the material and  $h_e$  is the coefficient of superficial thermal conduction.  $I_g$  is the global intensity of incident solar radiation, with values that are fixed and related to the location, position and schedule. The solar earnings were represented by the term  $\frac{K \alpha I_g}{h_e}$  and the factor of solar earnings by:  $\frac{K \alpha}{h_e}$ .

The coefficient of superficial thermal conductance ( $h_e$ ) values were adapted from Frota and Shiffer (a.b. Frota and s.r. Shiffer, 1988) and their fixed values take into account whether the walls position (vertical or horizontal) and, still, whether the flow (ascending or descending).

The construction of the global coefficient of thermal transmission was also in agreement with that one given by Frota and Shiffer (a.b. Frota and s.r. Shiffer, 1988).

$$\frac{1}{K} = \frac{1}{h_e} + \sum_{j=1}^n \frac{l_j}{k_j} + \frac{1}{h_i},$$

where  $1/h_e$  and  $1/h_i$  are the

outdoor and indoor superficial thermal resistances, respectively. For the case of walls composed by different materials, to each wall thickness ( $l$ ) the thermal conductivity ( $k$ ) of the respective material is associated and,  $j = 1 \dots n$ , being  $n$  the number of materials of which the wall is composed. Figure 8 presents the layers that form the covering flagstone.

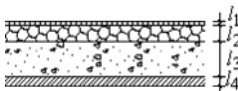
	LAYER	MATERIAL
	11	waterproof with clear painting
	12	concrete with expanded clay
	13	armed concrete
	14	painting roughcast

Figure 8 Layers that form the covering flagstone.

## RESULTS

Figures 9-11 present the results in terms of velocity wind field.

For a more comprehensive view of indoor air circulation an area (red square) was selected to be enlarged. We can observe from Figure 9, which represents the original project of wind fields, that the indoor environment presents poor ventilation. The fact that the introduction of the wind-catch, Figures 10 and 11, has significantly altered the wind field and suggests that its application deserves more investigation.

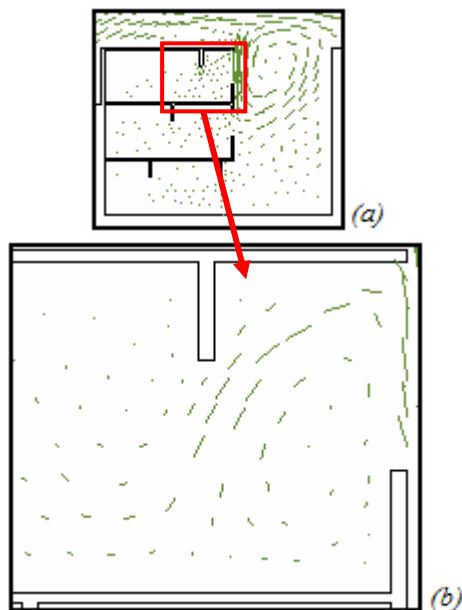


Figure 9 Detail of the velocity wind field of the original project (a) and a more detailed region (b).

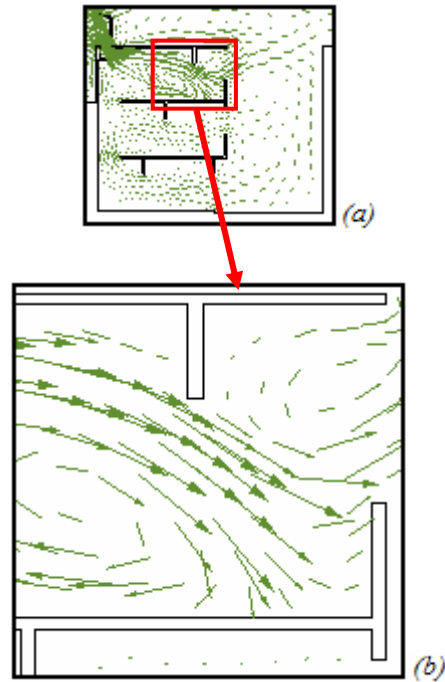


Figure 10 Detail of the velocity wind field - short wind-catch project (a) and a detailed region (b).

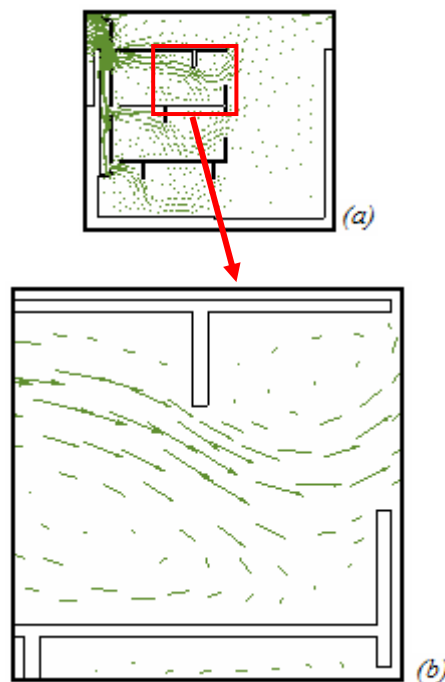


Figure 11 Detail of the velocity wind field - long wind-catch project (a) and a detailed region (b).

Now, these results were taken in terms of contour fill of  $|\mathbf{u}|$  in a scale in which the darkest colour will be adopted for superior velocities of 1.5 m/s in the colour scale (Figure 12). In order to compare the alterations made to the original project change, the same colour scale was adopted to show the results.



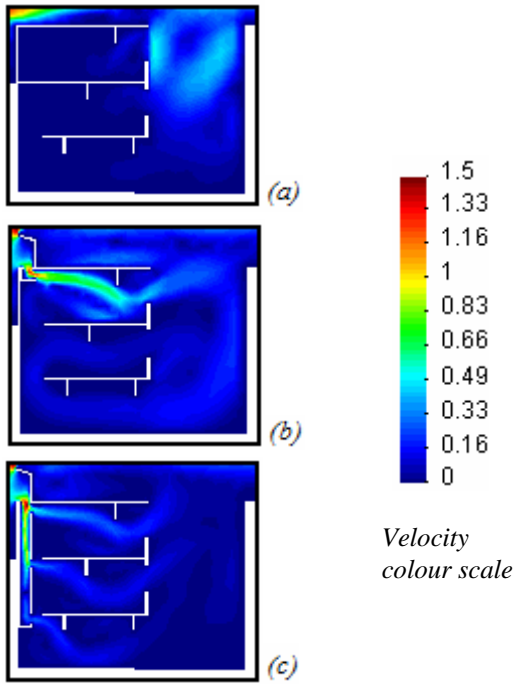


Figure 12 Contour fill of  $|u|$ . Original project (a), long wind-catch (b) and short wind-catch (c).

Figures 13-16 present the results in terms of contour fill of temperature plus display vectors for four analyzed situations; without incident solar radiation (Figure 13), with incident solar radiation related to 7 a.m. (Figure 14), incident solar radiation related to 12 a.m. (Figure 15) and incident solar radiation related to 4 p.m. (Figure 16). In order to compare the alterations made to the original project, the same color scale was adopted to show the results, in other words, including the same temperature strip.

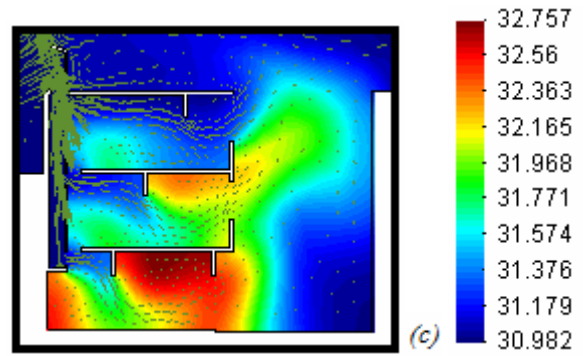


Figure 13 Contour fill of temperature without the interference of the incident solar radiation; original (a), short wind-catch (b), long wind-catch (c) and temperature colour scale.

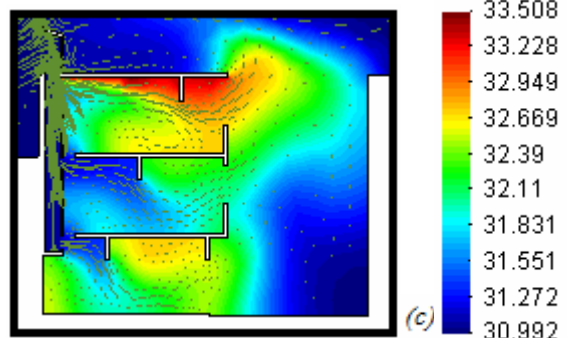
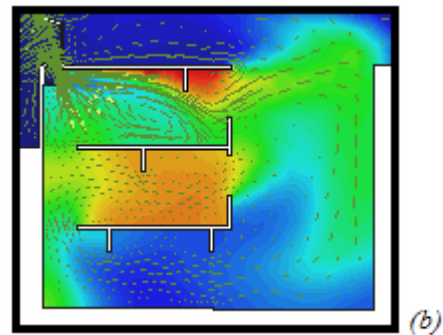
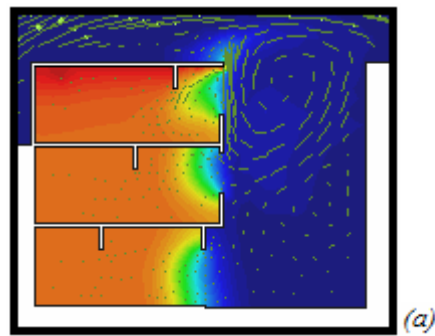
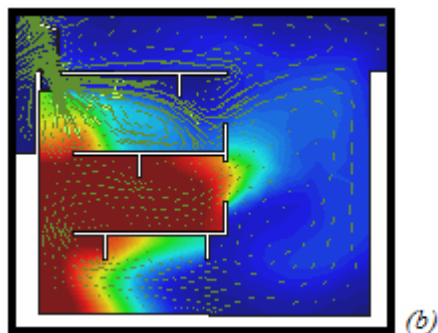
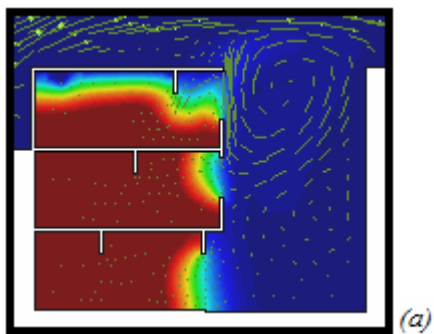


Figure 14 Contour fill of temperature with the interference of the incident solar radiation related to 7 a.m.; original (a), short wind-catch (b), long wind-catch (c) and temperature colour scale.



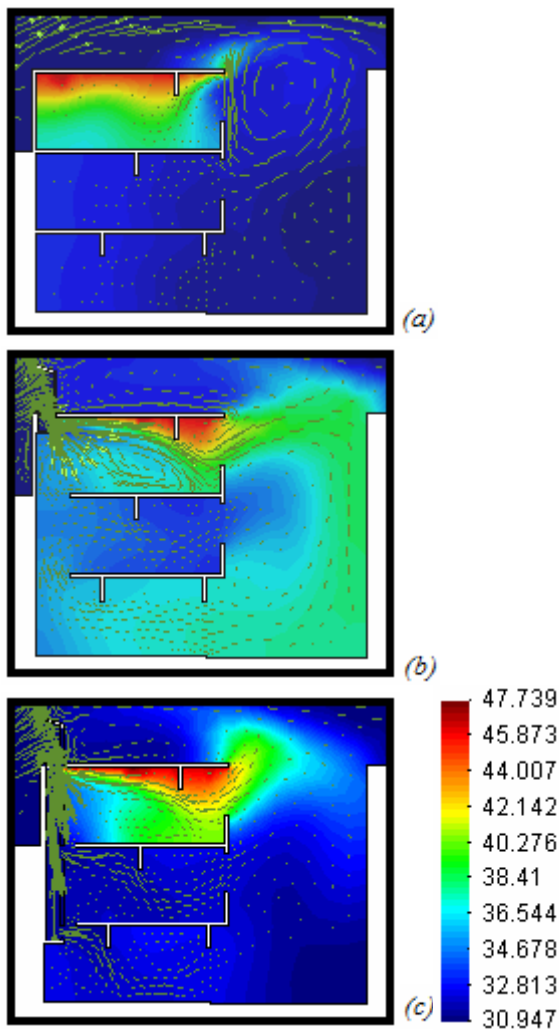


Figure 15 Contour fill of temperature with the interference of the incident solar radiation related to 12 a.m; original (a), short wind-catch (b), long wind-catch (c) and temperature colour scale.

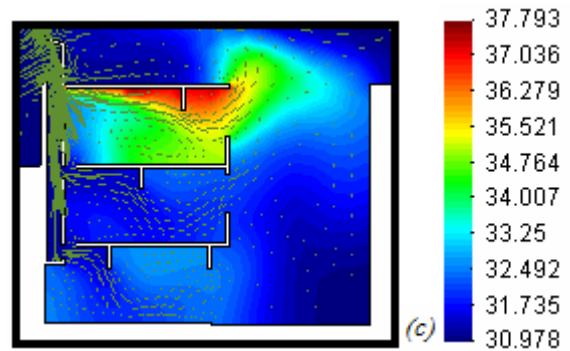
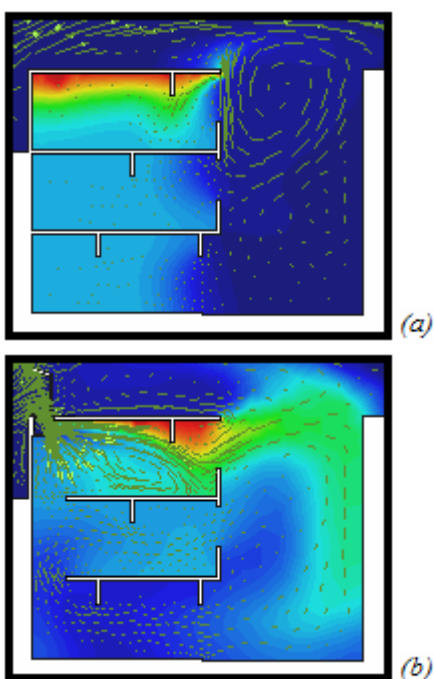


Figure 16 Contour fill of temperature with the interference of the incident solar radiation related to 4 a.m; original (a), short wind-catch (b), long wind-catch (c) and temperature colour scale.

The computational temperature results allow us to see the capacity of the system (wind-catch plus a studied arrangement of openings) to promote the indoor cooling.

## CONCLUSION

To analyze the air circulation problems, a mixed stabilized finite element method, like Petrov-Galerkin, was used. This allows us to deal with the problems that come from the equation system. It ensures stability for dominant advection and for the internal constraint. The application of the finite element method for space discretization in studies related to architecture and a town plan, presents as an advantage the fact that it is efficient when working with domains of complex geometries as well as with varied boundary conditions. By this method, it is possible to obtain punctual values of wind velocity, temperature and gas concentration in the areas of interest.

Regarding the original project, it is possible to notice the poor indoor ventilation in terms of distribution and intensity. Changes to the original are proposed project through the introduction of the wind-catch in two ways. Firstly by adding to a project a short wind-catch only on the third-floor. Secondly by introducing a long wind-catch that crosses all the building with openings on all floors. The computational experiments with both short wind-catch and long wind-catch brought positive results. It was possible to observe the increase in air circulation in terms of intensity and distribution and that the system was able to promote air circulation in the interior even when the outdoor wind was low, (1m/s). The results obtained from the heat problem suggest the capacity of changing indoor temperature by improving ventilation with a reasonable arrangement of openings.

The four analyzed situations allow us to observe indoor cooling for the new scenarios with wind-catch if compared to the original scenarios. In the cases without incident solar radiation (Figure 13) and with incident solar radiation related to 7 a.m. (Figure 14),

indoor temperatures reached values very close to the outdoor temperatures showing that the new opening was able to promote cooling by inducing a cross ventilation. For the two other situations such as the one related to 12 a.m. (Figure 15) and 4 p.m. (Figure 16) in which the indoor temperature reached values higher than the others cases, the action of the wind-catch was able to promote an expressive decrease of the indoor temperature. In the case of high temperatures, the ventilation was capable of interfering in the thermal sensation reducing the unpleasant sensation of heat. So, for the four presented cases, it can be observed that the introduction of the wind-catch, therefore the insertion of cross ventilation brought about won in quality for the indoor spaces.

If the analysis was focused on the interior of the house the results show an increase in the ventilation of all floors even when the short wind-catch was applied. Focusing the interest only on the third-floor it is possible to observe that with the short wind-catch the ventilation intensity is higher. Therefore, it will be a better choice because besides scarce ventilation this pavement receives solar radiation directly.

The computational results obtained here, confirming the North African vernacular architectural results, suggest that the utilization of wind-catch to improve ambient conditions deserves more attention and research, since these strategies show good potential in achieving significant quality with reduced environmental and economical costs.

### ACKNOWLEDGEMENT

The author thanks the National Council for Scientific and Technological Development (CNPq) for its support, and the National Laboratory for Scientific Computing, LNCC/MCT for making this work possible.

This work is part of the author's doctoral thesis under the supervision of Prof. José Karam Filho, D.Sci. - National Laboratory for Scientific Computing, LNCC/MCT.

### REFERENCES

- von der Weid, R. 2004. O bonde como elemento de expansão urbana no Rio de Janeiro. Setor de História da Fundação Casa de Rui Barbosa.
- Drach, P. R. C. 2007. Computational Modelling and Numerical Simulation in Architecture Aiming at Comfort of Building Environments. Ph.D. Thesis, National Laboratory for Scientific Computing, LNCC/MCT (Brazil), 286 pages.
- Drach, P. R. C., Karam F., J. 2008. Computational simulation of the temperature field behavior in a confined space: Interference of the incident solar radiation on flat roofs. In: Proceedings do EUROSUN 2008 – 1st International Conference

on Solar Heating, Cooling and Buildings, Lisboa, Portugal, 2008.

- Franca, L. P., Frey, S. L. 1992. Stabilized finite element methods: II. The incompressible Navier-Stokes equations. *Computer Methods in Applied Mechanics Engineering*. Vol. 99. pp 209-233.
- Brooks, A., Hughes, T. J. R. 1982. Streamline Upwind/Petrov-Galerkin formulations for convection dominated flows with particular emphasis on the incompressible Navier-Stokes equations. *Computer Methods in Applied Mechanics Engineering*. Vol. 32. pp 199-259.
- Frota, A. B., Shiffer, S. R. 1988. *Manual de Conforto Térmico*. Livraria Nobel, São Paulo.